The nuclear receptor hepatocyte nuclear factor 4α acts as a morphogen to induce the formation of microvilli

Hideki Chiba,[1] Naoyuki Sakai,[1] Masaki Murata,[1] Makoto Osanai,[1] Takafumi Ninomiya,[2] Takashi Kojima,[1] and Norimasa Sawada[1]

[1]Department of Pathology and [2]Department of Anatomy, Sapporo Medical University School of Medicine, Sapporo 060-8556, Japan

Microvilli are actin-based organelles found on apical plasma membranes that are involved in nutrient uptake and signal transduction. Numerous components, including ezrin/radixin/moesin (ERM) proteins, have been identified that link filamentous actins to transmembrane proteins, but the signals driving microvillus biogenesis are not known. In this study, we show that the conditional and/or ectopic expression of a nuclear receptor, hepatocyte nuclear factor 4α (HNF4α), triggers microvillus morphogenesis. We also demonstrate that HNF4α expression induces ERM-binding phosphoprotein 50 (EBP50) expression and that attenuation of EBP50 using RNA interference inhibits microvillus development. We conclude that HNF4α acts as a morphogen to trigger microvillus formation.

Introduction

Among the landmarks for apicobasal cell polarity, microvilli are actin-based protrusions on the apical surfaces of epithelial and sensory cells. In epithelia of the small intestine and kidney proximal tubule, closely packed microvilli known as the brush border are observed on their apical plasma membranes. They participate in a variety of functions such as nutrient absorption, mechanosensory transduction, and phototransduction. The core structure of microvilli is comprised of parallel actin filaments, and numerous actin-binding proteins, including villin, espin, fimbrin, fascin, and myosins as well as ezrin/radixin/moesin (ERM) proteins, have been identified as components of microvilli (for reviews see DeRosier and Tilney 2000; Bretscher et al., 2002; Frolenkov et al., 2004). Some transmembrane proteins such as Cad99C, the *Drosophila melanogaster* orthologue of the vertebrate procadherin 15 (D'Alterio et al., 2005; Schlichting et al., 2006), are also known to be constituents of microvilli.

ERM proteins (Bretscher, 1983; Lankes et al., 1988; Tsukita et al., 1989) bind not only to actin filaments at their C-terminal domains but also to various transmembrane proteins at their N-terminal 4.1 ERM domains, thereby acting as cross-linkers between the cytoskeleton and the plasma membrane (for reviews see Mangeat et al., 1999; Tsukita and Yonemura, 1999; Bretscher et al., 2002). Their N-terminal halves are also indirectly associated with membrane proteins through Na^+/H^+ exchanger regulatory factor 1/ERM-binding phosphoprotein 50 (EBP50; Weinman et al., 1995; Reczek et al., 1997; Reczek and Bretscher, 1998; Finnerty et al., 2004; for reviews see Bretscher et al., 2002; Donowitz et al., 2005). However, ERM proteins are known to exist in a dormant state in terms of their cross-linking activity, when the 4.1 ERM domains interact with their own C-terminal tail (Gary and Bretscher, 1995; Pearson et al., 2000). Phosphorylation on the conserved threonine residues in the C terminus (T567/T564/T568 in ezrin/radixin/moesin, respectively) is considered to cause conformational changes in ERM proteins, resulting in their activation to interact with other molecules (Matsui et al., 1998). The suppressed expression of ERM proteins in cultured cells by antisense oligonucleotides leads to the loss of microvilli, suggesting their functional significance in microvillus formation (Takeuchi et al., 1994). Although moesin-deficient mice show no obvious abnormalities (Doi et al., 1999), the absence of radixin causes the disappearance of microvilli in bile canalicular membranes of hepatocytes in mice (Kikuchi et al., 2002). In addition, ezrin knockout and knockdown mice as well as EBP50-deficient mice exhibit shortened and irregular microvilli in enterocytes with differences in their extent

Correspondence to Hideki Chiba: hidchiba@sapmed.ac.jp

Abbreviations used in this paper: Dox, doxycycline; EBP50, ERM-binding phosphoprotein 50; ERM, ezrin/radixin/moesin; HNF4α, hepatocyte nuclear factor 4α; RARγ, retinoic acid receptor γ; RLE, rat lung endothelial; RXRα, retinoid X receptor α; tRA, all-trans retinoic acid; WT, wild type.

The online version of this article contains supplemental material.

The Journal of Cell Biology, Vol. 175, No. 6, December 18, 2006 971–980
http://www.jcb.org/cgi/doi/10.1083/jcb.200608012

(Morales et al., 2004; Saotome et al., 2004; Tamura et al., 2005), indicating their important roles in microvillus development. Thus, although molecular constituents of microvilli and their interactions have been disclosed, it remains obscure which signals cue microvillus morphogenesis.

Hepatocyte nuclear factor 4α (HNF4α), a member of the nuclear receptor superfamily, transcriptionally regulates the expression of many target genes involved in glucose, fatty acid, amino acid, ammonia, cholesterol, steroid, and drug metabolism as well as in hematopoiesis and blood coagulation (Sladek et al., 1990; Li et al., 2000; Hayhurst et al., 2001; Tirona et al., 2003; for reviews see Sladek and Seidel, 2001; Watt et al., 2003). During early development, it is initially detected in primitive endoderm cells and afterward is expressed in visceral endoderm cells (Duncan et al., 1994), which cover the fetal components and possess various properties similar to those in hepatocytes (for review see Watt et al., 2003). In the adult, HNF4α is expressed in several types of epithelial cells, such as hepatocytes, enterocytes, β cells of the pancreas, and proximal tubular epithelia in the kidney, and is reported to contribute to the differentiation of these cells. Several lines of evidence have made it clear that HNF4α also plays an essential role in activation of the expression of genes encoding cell junction molecules (Späth and Weiss, 1998; Chiba et al., 2003; Parviz et al., 2003; Satohisa et al., 2005; Battle et al., 2006). In addition, recent studies using four distinct cell lines have shown that HNF4α is implicated in the control of cell proliferation (Lazarevich et al., 2004; Chiba et al., 2005; Lucas et al., 2005). Moreover, chromatin immunoprecipitation combined with promoter microarrays has revealed that HNF4α occupies an exceptionally huge number of promoters in human hepatocytes and pancreatic islets, implying its broad range of physiological functions.

Mouse F9 embryonal carcinoma cells show no or little spontaneous differentiation when cultured in the absence of retinoic acid. Conversely, those grown as monolayers and aggregates differentiate upon retinoic acid treatment into primitive endoderm– and visceral endoderm–like cells, respectively, both of which represent polarized epithelial cells bearing junctional complexes (Hogan et al., 1981; Strickland, 1981). Judging from these properties, F9 cells are regarded as an attractive system to study the molecular mechanisms not only of early embryonic development, cell differentiation, and retinoid signaling but also of the organization of cell junctions and epithelial polarity. To facilitate the study of gene functions of interest in F9 cells, we previously established the cell line F9:rtTA:Cre-ER^{T} L32T2 (also called F9 L32T2), which allows sophisticated genetic manipulation such as the sequential inactivation of *loxP*-flanked genes and strict regulation of gene expression without altering its general characteristics (Chiba et al., 2000).

We subsequently generated F9 cells expressing doxycycline (Dox)-inducible HNF4α (F9 L32T2:HNF4α) and found that HNF4α triggered the expression of several tight-junction molecules as well as the establishment of cell–cell junctions and epithelial polarity (Chiba et al., 2003; Satohisa et al., 2005). Therefore, we hypothesized that HNF4α might also be involved in microvillus morphogenesis. To test this assumption, we used F9 L32T2:HNF4α and the rat lung endothelial (RLE) cell line RLE:rtTA:HNF4α, in which HNF4α expression is also conditionally induced by Dox (Chiba et al., 2005). Our study highlights that HNF4α provokes microvillus biogenesis as a morphogen via the induction of EBP50 expression. We also compared the phenotype in retinoid X receptor α (RXRα)/retinoic acid receptor γ (RARγ)–deficient F9 cells (Chiba et al., 1997a; Kubota et al., 2001) with that in wild-type (WT) cells and determined the functional relevance of retinoid receptors in microvillus formation. Furthermore, we examined whether the up-regulation of EBP50 was sufficient for the morphogenesis of microvilli in F9 cells.

Results

HNF4α initiates microvillus formation in F9 cells

By scanning and transmission electron microscopy, we first determined whether microvillus formation was also induced in the cells. In undifferentiated cells grown in the absence of Dox, filopodia- and lamellipodia-like structures were observed, but there were few microvilli (Fig. 1, A and B; top). On the other hand, in F9 L32T2:HNF4α cells treated for 72 h with 1 μg/ml

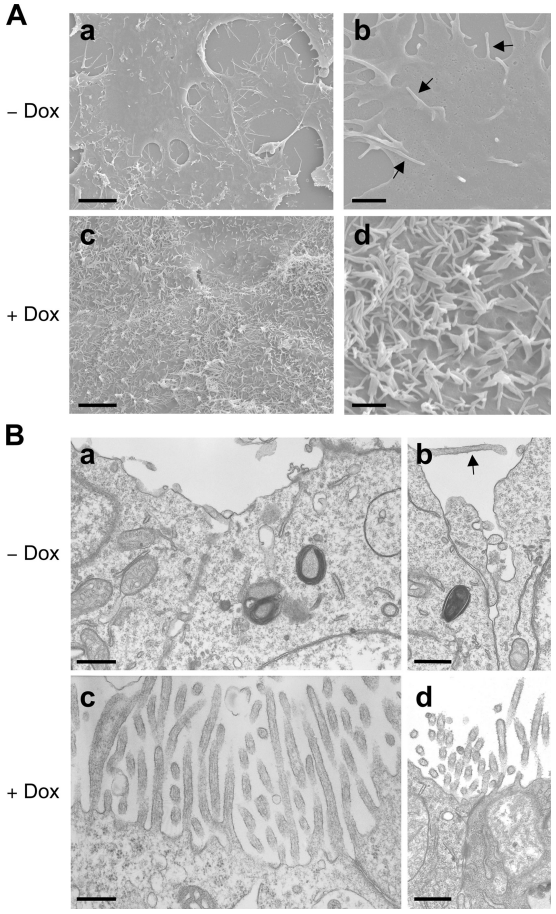

Figure 1. **Scanning and transmission electron micrographs of F9 cells expressing Dox-inducible HNF4α.** F9 L32T2:HNF4α clone 8 cells were treated for 72 h with either the vehicle (A and B, top) or 1 μg/ml Dox (A and B, bottom). They were examined under scanning (A) and transmission (B) electron microscopes. Arrows indicate filopodia-like structures. Bars (A, a and c), 5 μm; (A, b and d), 1 μm; (B), 500 nm.

Dox, the number of microvilli, which contained parallel actin filaments, was strikingly increased on the apical cell surfaces and along the cell borders (Fig. 1, A and B; bottom). Note that the majority of the Dox-exposed cells exhibited microvilli with variations in number and length and that tightly packed arrays of microvilli were frequently detected.

HNF4α induces EBP50 expression in F9 cells

Because HNF4α provoked microvillus biogenesis in F9 cells, we hypothesized that HNF4α may induce the gene expression of microvillus components such as ERM proteins and EBP50. As shown in Fig. 2, the expression of EBP50 mRNA was activated in F9 cell lines expressing Dox-induced HNF4α. The levels of EBP50 transcripts in F9 L32T2:HNF4α cells were elevated by Dox in time- and dose-dependent manners in terms of the amount of HNF4α (for HNF4α expression, see Chiba et al., 2003, 2005) and were three- to fourfold higher in the cells treated for 48 h with 1 μg/ml Dox than in the cells grown without Dox exposure. In contrast, the expression of ezrin, radixin, and moesin mRNAs was marginally altered in the cells after Dox treatment.

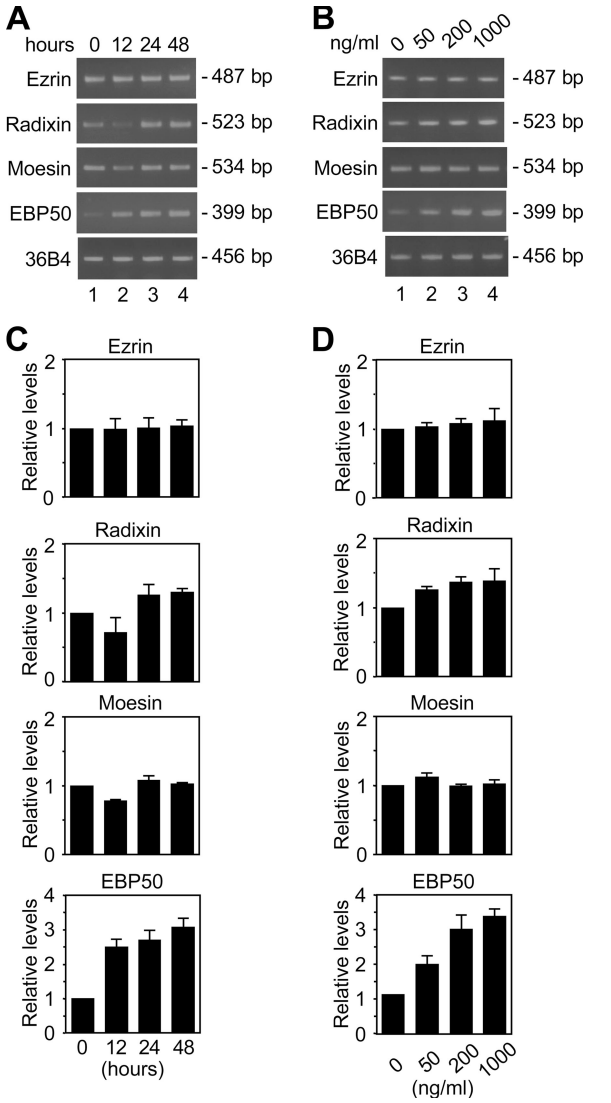

Figure 2. **Activation of expression of the *EBP50* gene in F9 cells expressing Dox-induced HNF4α.** (A) F9 L32T2:HNF4α clone 8 cells were exposed to 1 μg/ml Dox for 0, 12, 24, and 48 h (lanes 1, 2, 3, and 4, respectively). 1 μg of total RNA from the cells was subjected to RT-PCR analysis for the indicated genes. PCR was performed for 17 (36B4), 22 (ezrin, radixin, and EBP50), or 23 (moesin) cycles. (B) Cells were treated for 48 h with 0, 50, 200, and 1,000 ng/ml Dox (lanes 1, 2, 3, and 4, respectively). PCR was performed as in A. (C and D) RT-PCR analysis was performed as in A and B for three independent experiments. The mRNA levels were normalized to the corresponding 36B4 levels and expressed relative to the amount present in cells grown in the absence of Dox, which was taken as 1. Values represent the mean ± SD (error bars; $n = 3$).

By Western blot analysis, we subsequently checked the expression levels of these four microvillus proteins as well as that of villin in F9 L32T2:HNF4α cells. EBP50 protein was abundantly induced in the cells after 24 and 48 h of 1 μg/ml Dox treatment (approximately 6- and 11–15-fold increases, respectively; Fig. 3, A and B). In addition, the level of EBP50 protein appeared to be increased by Dox and, thereby, HNF4α in a dose-dependent fashion (Fig. 3 B). The expression of villin was moderately induced in the cells (Fig. S1, A and B; available at http://www.jcb.org/cgi/content/full/jcb.200608012/DC1), as reported for human embryonic kidney cells expressing HNF4α (Lucas et al., 2005). In contrast, little or no change in the expression levels of ezrin or moesin was observed in the cells after Dox exposure, and radixin expression was only weakly increased in cells treated for 48 h with 1 μg/ml Dox (1.5–2-fold increase). Together with the data of RT-PCR analysis, these results indicated that HNF4α extensively activated the expression of EBP50.

ERM proteins are phosphorylated and apically concentrated in F9 cells expressing HNF4α

ERM proteins are reported to be activated after phosphorylation at the conserved C-terminal threonine residues (T567/T564/T558 residues in ezrin/radixin/moesin, respectively) in order to interact with other molecules (Matsui et al., 1998; for review see Bretscher et al., 2002). Therefore, by immunoblotting with an antibody against the phospho–ezrin (T567)/radixin (T564)/moesin (T558), we next analyzed the phosphorylation states of ERM proteins in F9 L32T2:HNF4α cells (Fig. 4 A). The threonine-phosphorylated ERM proteins were barely detected in the cells grown without Dox, whereas their levels were extremely increased in the cells exposed for 72 h to 1 μg/ml Dox (about a 70-fold increase). On the other hand, the amounts of ezrin, radixin, and moesin were not largely altered after Dox treatment. Thus, ERM proteins were heavily phosphorylated on the conserved C-terminal threonine residues in F9 cells expressing Dox-induced HNF4α.

We then examined the distribution of ezrin, radixin, moesin, phospho-ERM, EBP50, and villin in F9 L32T2:HNF4α cells by immunostaining. In the cells exposed for 72 h to 1 μg/ml Dox, these proteins were concentrated on the apical cell surfaces and cell boundaries in a dotlike manner, which was consistent with the localization pattern of microvilli (Fig. 4 B). Ezrin, radixin, moesin, and EBP50 proteins were also colocalized, at least in part, with filamentous actin (Fig. 4 C). Conversely, in

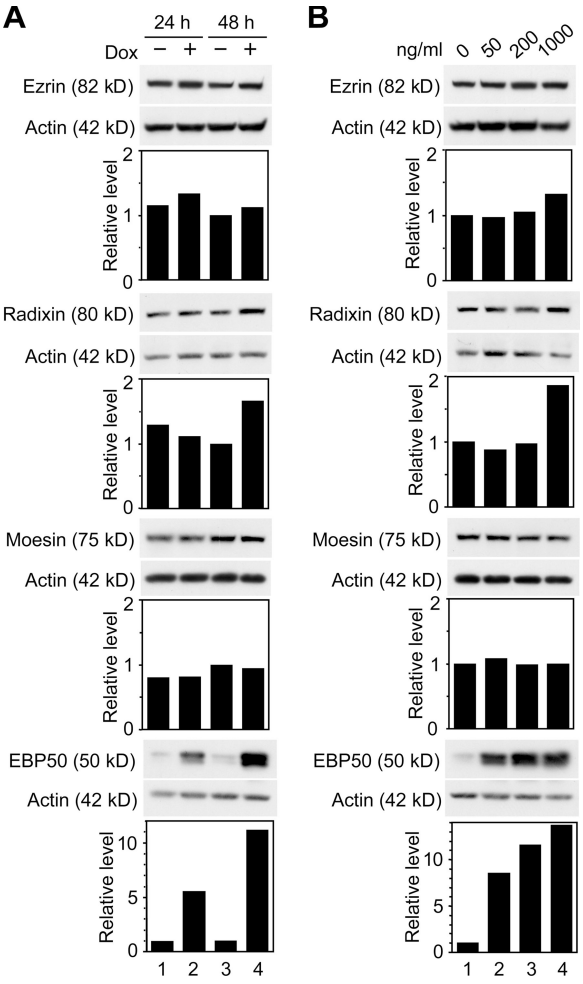

Figure 3. **Induction of the expression of EBP50 protein in F9 cells expressing Dox-induced HNF4α.** (A) F9 L32T2:HNF4α clone 8 cells were treated with the vehicle (lanes 1 and 3) or 1 μg/ml Dox (lanes 2 and 4) for 24 (lanes 1 and 2) and 48 h (lanes 3 and 4). 25 μg of whole cell extract from the cells was separated by SDS-PAGE and immunoblotted with the corresponding antibodies followed by chemiluminescence detection. Each blot was stripped and reimmunoprobed with an antiactin antibody. The protein levels were normalized to the corresponding actin levels and expressed relative to the amount present in cells exposed for 48 h to the vehicle, which was taken as 1. (B) Cells were treated for 48 h with 0, 50, 200, and 1,000 ng/ml Dox (lanes 1, 2, 3, and 4, respectively). Western blot analysis was performed, and the protein levels were expressed as in A.

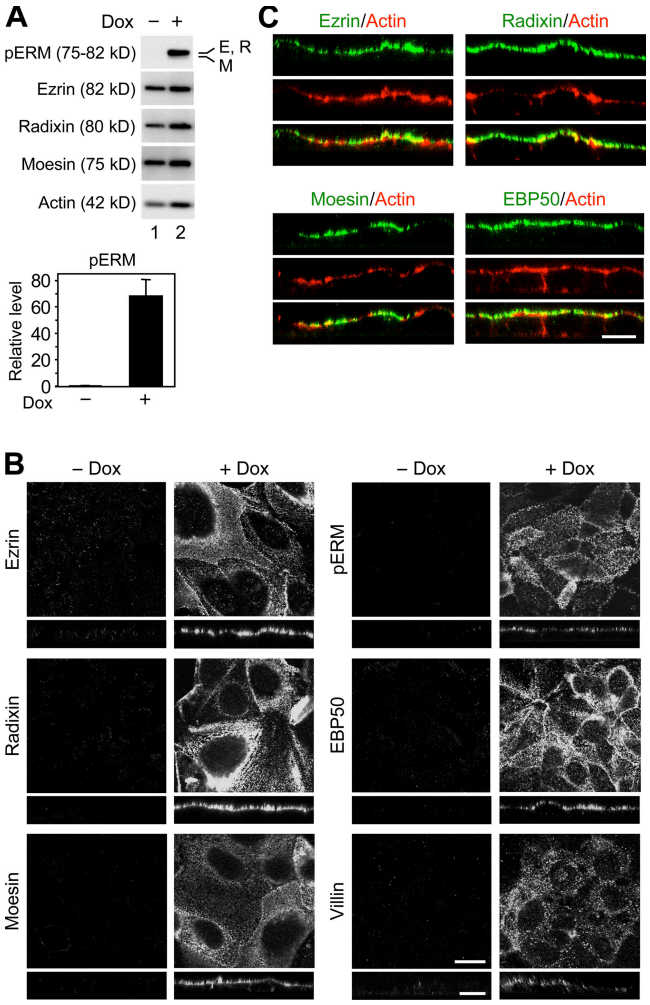

Figure 4. **Phosphorylation and apical concentration of ERM proteins in F9 cells expressing Dox-induced HNF4α.** (A) F9 L32T2:HNF4α clone 8 cells were treated for 72 h with the vehicle (lane 1) or 1 μg/ml Dox (lane 2). 25 μg of whole cell extract from the cells was separated by SDS-PAGE and immunoblotted with the corresponding antibodies followed by chemiluminescence detection. E, ezrin; R, radixin; M, moesin. Western blot analysis of threonine-phosphorylated ERM (pERM) proteins was performed for four independent experiments. The signal intensities were normalized to the corresponding actin levels and expressed relative to the amount present in cells exposed for 72 h to the vehicle, which was taken as 1. The values represent the mean ± SD (error bars; $n = 4$). (B and C) Cells were grown for 72 h in the presence or absence of 1 μg/ml Dox. They were subjected to immunostaining with the corresponding antibodies, and their x-y images of apical cell surfaces and z-section images were observed under a laser-scanning confocal microscope. Bars, 20 μm.

the cells grown without Dox, they showed neither apical enrichment nor any specific subcellular distribution except moesin exhibiting weak positive signals along lateral and apical plasma membranes (Fig. 4 B).

HNF4α-induced EBP50 plays a key role in microvillus morphogenesis in F9 cells

In villin-deficient mice, no gross abnormalities are observed in microvillus formation (Pinson et al., 1998; Ferrary et al., 1999). Therefore, the important question that arises from the aforementioned results is whether HNF4α-induced EBP50 expression is required for the phosphorylation and apical concentration of ERM proteins as well as microvillus formation. To address this issue, we used an RNAi approach to knock down the expression of EBP50. F9 L32T2:HNF4α cells were transfected with the siRNAs against EBP50 or negative control siRNA and were incubated for 6 h after transfection followed by treatment for 72 h with 1 μg/ml Dox. Western blot analysis revealed that the three distinct EBP50 siRNAs effectively reduced the EBP50 expression (Fig. 5 A). Importantly, when the expression of EBP50 was suppressed in the cells, the levels of threonine-phosphorylated ERM proteins were strongly decreased, whereas total amounts of ezrin, radixin, and moesin were basically not affected (Fig. 5 A). In addition, the reduction of EBP50 expression in the cells resulted in impairment of the apical enrichment of ezrin and radixin (Fig. 5 B). Moreover, the knockdown of EBP50 expression led to a remarkable decrease in both the

number and length of microvilli on the apical cell surface (Fig. 5 C). Altogether, these results indicated that HNF4α triggered the phosphorylation and apical concentration of ERM proteins as well as microvillus morphogenesis through the up-regulation of EBP50 expression.

Ectopically induced HNF4α triggers the biogenesis of microvilli-like structures and EBP50 expression in endothelial cells

To elucidate whether the induction of HNF4α causes microvillus biogenesis in another type of cell, we subsequently used the vascular endothelial cell line RLE:rtTA:HNF4α, in which HNF4α expression was induced by Dox treatment as described previously (Chiba et al., 2005). On scanning electron microscopy, only a small number of fingerlike protrusions were detected on apical surfaces of the cells grown in the absence of Dox (Fig. 6 A, top). In contrast, in the cells exposed for 72 h to 1 μg/ml Dox, the number and length of microvilli-like structures were extremely increased (Fig. 6 A, bottom) as in the Dox-treated F9 L32T2:HNF4α cells. On transmission electron microscopy, however, parallel actin bundles were not apparent in fingerlike extensions of the Dox-exposed cells (Fig. 6 B). Furthermore, the expression of EBP50 and villin was induced in the cells after 24 and 48 h of 1 μg/ml Dox treatment, and its levels were elevated by Dox in a dose-dependent manner (Fig. 6, C–E; for HNF4α expression, see Chiba et al., 2005). On the other hand, the expression of ezrin, radixin, and moesin was not grossly changed in the cells after Dox exposure. Immunostaining showed that ezrin, phospho-ERM, EBP50, and villin were apically enriched in the cells treated for 72 h with 1 μg/ml Dox but not in the vehicle-treated cells (Fig. S2, available at http://www.jcb.org/cgi/content/full/jcb.200608012/DC1).

Retinoid receptors alone mediate the control of ezrin expression and weakly contribute to microvillus formation in F9 cells

We previously reported that retinoid receptors like HNF4α induced the gene expression of the same tight-junction molecules (occludin, claudin-6, and claudin-7) as well as the formation of functional tight junctions and epithelial polarity (Kubota et al., 2001; Chiba et al., 2003; Satohisa et al., 2005). Therefore, we investigated whether retinoid receptors contributed to microvillus formation. To this end, we used WT and RXRα$^{-/-}$/RARγ$^{-/-}$ F9 cells, the latter of which are defective for differentiation into epithelial cells (Chiba et al., 1997a; Kubota et al., 2001). Scanning electron microscopy showed that in WT cells treated for 96 h with 10^{-6} M all-trans retinoic acid (tRA), a small number of short microvilli developed on the apical-free surfaces (Fig. 7 A, top; arrows). On the other hand, in the tRA-exposed RXRα$^{-/-}$/RARγ$^{-/-}$ cells, microvilli were hardly observed (Fig. 7 A, bottom). Note that the number of microvilli was increased in the tRA-treated WT F9 cells compared with that of the vehicle-treated WT cells and the tRA-exposed RXRα$^{-/-}$/RARγ$^{-/-}$ cells (Fig. 7 A, b and d; and not depicted), although it was much smaller than on F9 L32T2:HNF4α cells treated with Dox (Fig. 1).

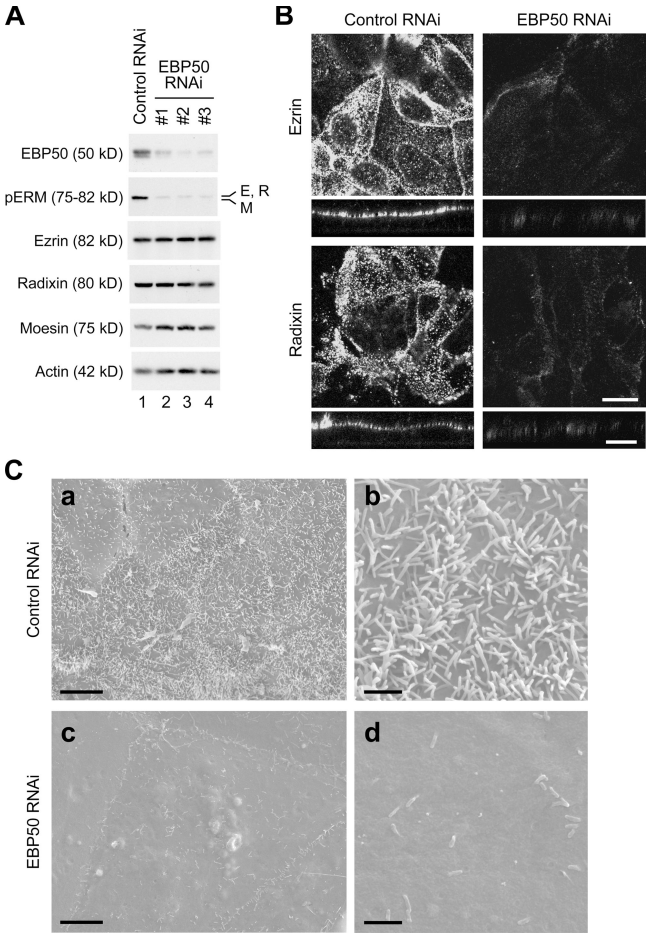

Figure 5. **Suppression of EBP50 expression prevents the phosphorylation and apical concentration of ERM proteins as well as microvillus biogenesis in F9 cells expressing Dox-induced HNF4α.** (A) F9 L32T2:HNF4α clone 8 cells were transfected with negative control siRNA (lane 1) or three distinct siRNAs against EBP50 (#1–3; lanes 2–4, respectively), incubated for 6 h after transfection, and then treated for 72 h with 1 μg/ml Dox. 25 μg of whole cell extract from the cells was separated by SDS-PAGE and immunoblotted with the corresponding antibodies followed by chemiluminescence detection. E, ezrin; R, radixin; M, moesin. (B) Cells were transfected with negative control siRNA or the EBP50 siRNA #2 and were incubated for 6 h after transfection followed by treatment for 72 h with 1 μg/ml Dox. They were subjected to immunostaining with the corresponding antibodies, and their x-y images of apical cell surfaces and z-section images were observed under a laser-scanning confocal microscope. (C) Cells were transfected and grown as in B and were examined under a scanning electron microscope. Bars (B), 20 μm; (C, a and c), 5 μm; (C, b and d), 1 μm.

We also examined the expression of ezrin, radixin, moesin, EBP50, and villin in WT and RXRα$^{-/-}$/RARγ$^{-/-}$ F9 cells. As shown in Fig. 7 (B and C) and Fig. S1 C, the expression of ezrin but not radixin, moesin, EBP50, or villin was induced in WT cells after 48 h of 10^{-6} M tRA treatment and was dose-dependently increased in the cells by tRA. Interestingly, no induction of ezrin expression was detected in the tRA-exposed RXRα$^{-/-}$/RARγ$^{-/-}$ cells (Fig. 7 D), indicating that retinoid signals for the induction of ezrin expression were mediated by these retinoid receptors. Moreover, ERM proteins were barely phosphorylated in WT F9 cells exposed for 96 h to 10^{-6} M tRA compared with the Dox-treated F9 L32T2:HNF4α cells (Fig. 7 E).

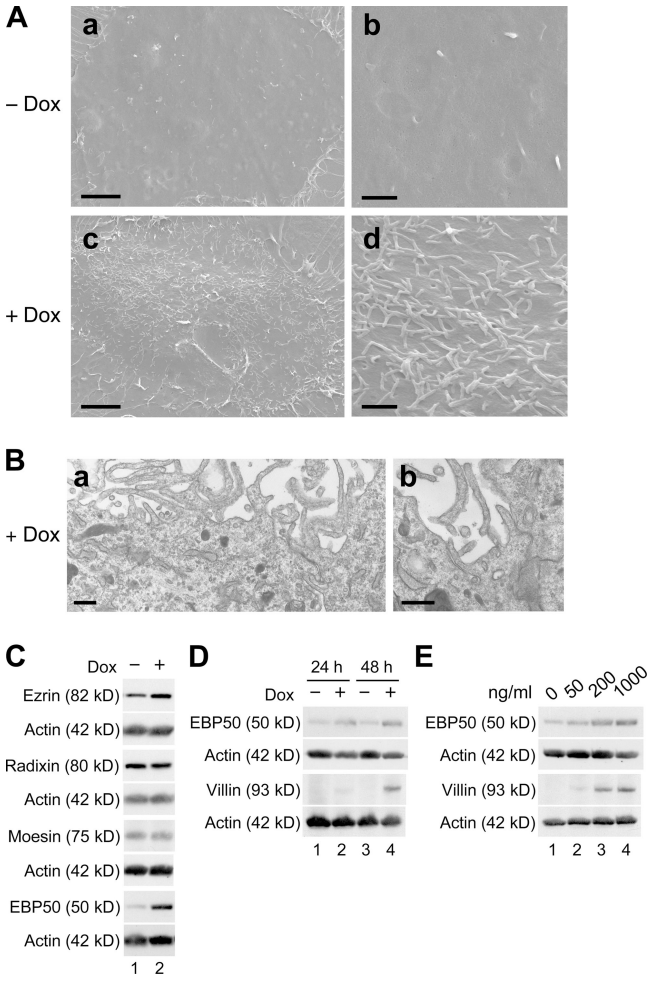

Figure 6. **Microvillus morphogenesis and EBP50 up-regulation in RLE cells expressing Dox-inducible HNF4α.** (A) RLE:rtTA:HNF4α clone 23 cells were treated for 72 h with either the vehicle (top) or 1 μg/ml Dox (bottom) and were examined under a scanning electron microscope. (B) Cells were exposed to 1 μg/ml Dox for 72 h and were examined under a transmission electron microscope. (C) Cells were treated for 48 h with either the vehicle (lane 1) or 1 μg/ml Dox (lane 2). 25 μg of whole cell extract from the cells was separated by SDS-PAGE and immunoblotted with the corresponding antibodies followed by chemiluminescence detection. Each blot was stripped and reimmunoprobed with an antiactin antibody. (D) Cells were treated for 24 (lanes 1 and 2) and 48 h (lanes 3 and 4) with either the vehicle (lanes 1 and 3) or 1 μg/ml Dox (lanes 2 and 4). (E) Cells were treated for 48 h with 0, 50, 200, and 1,000 ng/ml Dox (lanes 1, 2, 3, and 4, respectively). (D and E) Western blot analysis was performed as in C. Bars (A, a and c), 5 μm; (A, b and d), 1 μm; (B), 500 nm.

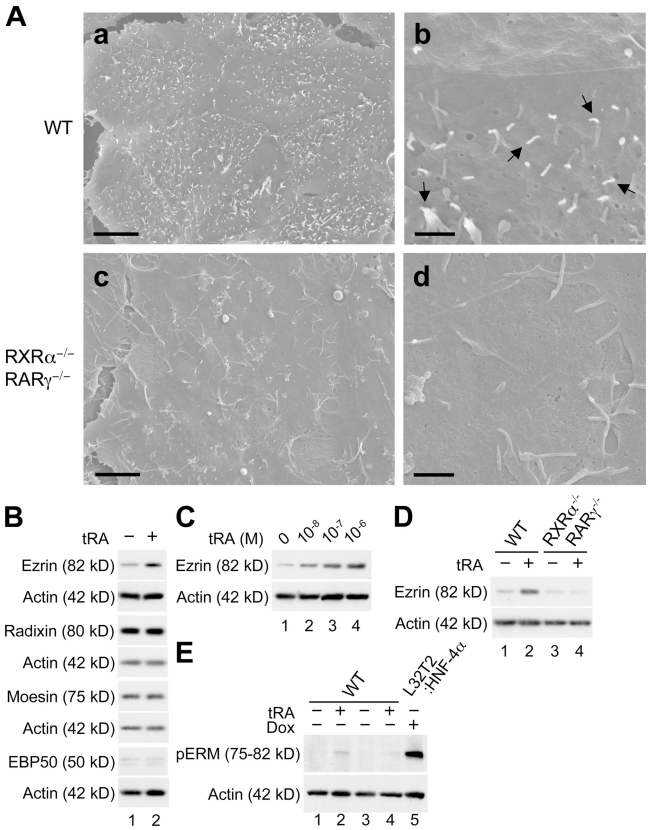

Figure 7. **Retinoid receptors mediate the induction of ezrin expression but weakly contribute to microvillus biogenesis in F9 cells.** (A) Wild-type (WT; top) and RXRα$^{-/-}$/RARγ$^{-/-}$ (bottom) F9 cells were treated for 96 h with 10^{-6} M tRA and were examined under a scanning electron microscope. Arrows indicate microvilli. Bars (a and c), 5 μm; (b and d), 1 μm. (B) WT F9 cells were treated for 48 h with either the vehicle (lane 1) or 10^{-6} M tRA (lane 2). 25 μg of whole cell extract from the cells was separated by SDS-PAGE and immunoblotted with the corresponding antibodies followed by chemiluminescence detection. Each blot was stripped and reimmunoprobed with an antiactin antibody. (C) WT F9 cells were treated for 48 h with 0, 10^{-8}, 10^{-7}, and 10^{-6} M tRA (lanes 1, 2, 3, and 4, respectively). (D) WT (lanes 1 and 2) and RXRα$^{-/-}$/RARγ$^{-/-}$ (lanes 3 and 4) F9 cells were treated for 48 h with either the vehicle (lanes 1 and 3) or 10^{-6} M tRA (lanes 2 and 4). (E) WT F9 cells were treated for 96 h with either the vehicle (lanes 1 and 3) or 10^{-6} M tRA (lanes 2 and 4). F9 L32T2:HNF4α clone 8 cells exposed for 72 h to 1 μg/ml Dox (lane 5) were used as a positive control. (C–E) Western blot analysis was performed as in B.

EBP50 triggers the activation of ERM proteins and microvillus morphogenesis in F9 cells treated with retinoic acid

We subsequently determined whether EBP50 overexpression was sufficient for microvillus formation in F9 cells. When F9 cells were transfected with EBP50 cDNA, little or no phospho-ERM protein was detected (Fig. 8 A). Interestingly, ERM proteins were phosphorylated when the EBP50 transfectants were exposed to 10^{-6} M tRA for 72 h, although their signals were relatively weak compared with those in the Dox-treated F9 L32T2:HNF4α cells, most probably because partial fractions of F9 cells were transfected with EBP50. In addition, ezrin, villin, and phospho-ERM proteins as well as EBP50 appeared to be apically concentrated in EBP50-overexpressed cells that were grown in the presence of tRA, whereas they were only sparsely detected on the apical cell surfaces in the tRA-treated nontransfectants (Fig. 8 B and Fig. S3 A, available at http://www.jcb.org/cgi/content/full/jcb.200608012/DC1). In the vehicle-exposed transfectants, EBP50 and ezrin but not villin or phospho-ERM were observed in a dotlike pattern at a different height of multilayer of the cells (Fig. 8 B, Fig. S3 A, and not depicted). Furthermore, on scanning electron microscopy, well-developed microvilli were observed on apical cell surfaces of EBP50 transfectants exposed to 10^{-6} M tRA for 96 h but not in the vehicle-treated nontransfectants (Fig. 8 C). The number and length of microvilli were fewer and shorter in both vehicle-treated transfectants and tRA-exposed nontransfectants than those observed in the tRA-treated transfectants (Fig. S3).

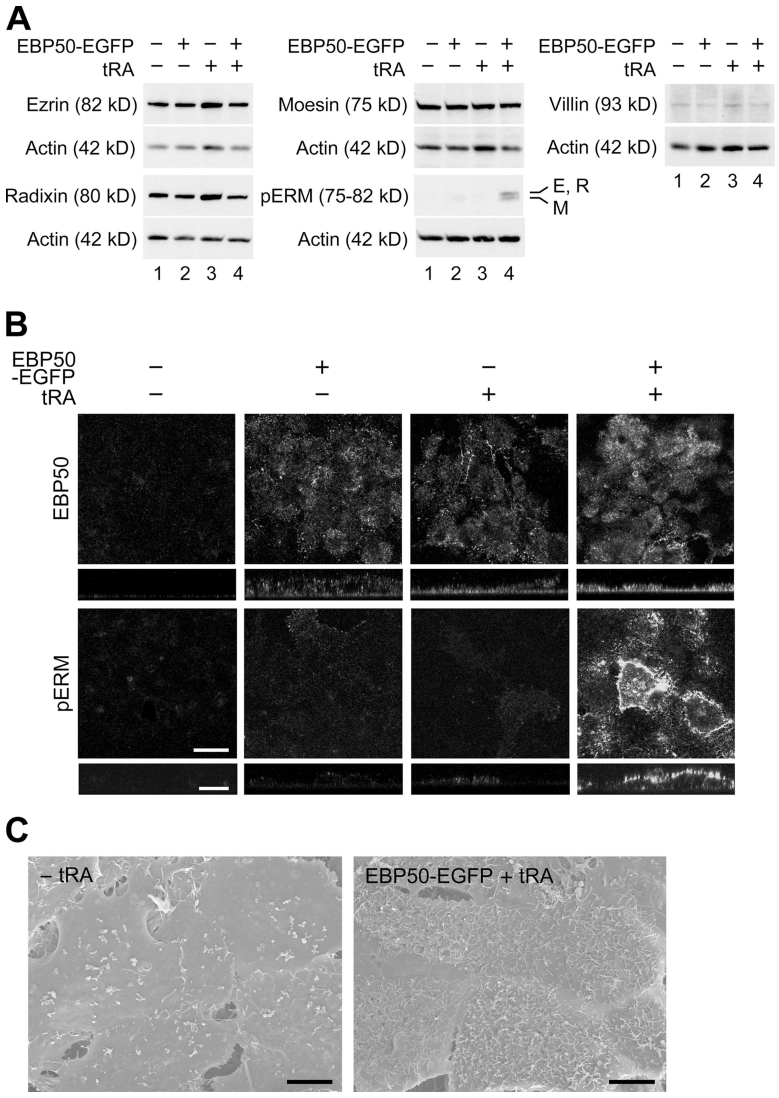

Figure 8. **EBP50 provokes the phosphorylation and apical concentration of ERM proteins as well as microvillus formation in retinoic acid–treated F9 cells.** (A) F9 L32T2:HNF4α clone 8 cells were transfected with the empty vector (lanes 1 and 3) or the EBP50-EGFP expression vector (lanes 2 and 4), incubated for 6 h after transfection, and treated for 72 h with either vehicle or 10^{-6} M tRA. 25 μg of whole cell extract from the cells was separated by SDS-PAGE and immunoblotted with the corresponding antibodies followed by chemiluminescence detection. Each blot was stripped and reimmunoprobed with an antiactin antibody. E, ezrin; R, radixin; M, moesin. (B) Cells were transfected and grown as in A. They were subjected to immunostaining with the corresponding antibodies, and their x-y images of apical cell surfaces and z-section images were observed under a laser-scanning confocal microscope. (C) Cells were transfected as in A and were exposed to either vehicle or 10^{-6} M tRA for 96 h. They were examined under a scanning electron microscope. Bars (B), 20 μm; (C), 5 μm.

Collectively, these results strongly suggest that the up-regulation of not only EBP50 but also other molecules that could be induced by retinoid receptors are required for HNF4α-triggered microvillus morphogenesis.

Discussion

We and others previously showed that HNF4α activated the expression of cell adhesion molecules, resulting in the acquisition of epithelial cell polarity and junctional complexes (Chiba et al., 2003; Parviz et al., 2003; Satohisa et al., 2005; Battle et al., 2006). In the present study, we have demonstrated by scanning and transmission electron microscopy that HNF4α also provokes the biogenesis of microvilli in F9 cells. In addition, the ectopic expression of HNF4α in the vascular endothelial cell line RLE initiated the development of apical fingerlike protrusions, although these did not bear visible parallel actin bundles. Because HNF4α is known to be expressed in epithelial cells such as enterocytes, proximal tubular epithelia, and hepatocytes, in which well-developed microvilli are observed, it may also be involved in microvillus organization in these cells. The importance of HNF4α in microvillus formation is supported by the observation that microvilli are absent in the bile canaliculi of hepatocytes in mice with conditional knockout of the *HNF4α* gene (Parviz et al., 2003). Thus, we concluded that HNF4α played a fundamental role not only in cell junction formation but also in microvillus morphogenesis, establishing at least two aspects of apicobasal cell polarity. It should also be noted that HNF4α-induced microvilli in F9 cells possessed some variations in number and length compared with the brush border-type microvilli in vivo. This might be explained by differences in the differentiation stages of epithelial cells derived from F9 stem cells.

One of the best-known mechanisms that activates ERM proteins as cross-linkers is phosphorylation on the conserved threonine residues in the C terminus (Gary and Bretscher, 1995; Matsui et al., 1998; Pearson et al., 2000; for reviews see Tsukita and Yonemura, 1999; Bretscher et al., 2002). We have indeed shown that ERM proteins appear to be heavily phosphorylated at the threonine residues and apically concentrated during the HNF4α-initiated formation of microvilli in F9 cells. This finding reinforces the notion that ERM proteins become activated

and exhibit asymmetrical subcellular localization via their phosphorylation to perform their functions.

Our results also revealed that the expression of EBP50 was induced by HNF4α in F9 L32T2:HNF4α and RLE:rtTA:HNF4α cells, whereas that of ezrin, radixin, and moesin was marginally altered in these cells. We examined the published gene array data and found that EBP50 expression is reduced in the HNF4α-null embryonic liver (Battle et al., 2006). More importantly, we found that the suppression of EBP50 expression by RNAi in F9 L32T2:HNF4α cells hindered threonine phosphorylation and apical enrichment of ERM proteins as well as microvillus biogenesis. These findings clearly indicated that HNF4α activated ERM proteins and drove microvillus morphogenesis via the induction of EBP50. In other words, the expression of EBP50 is required for both the activation of ERM proteins and the formation of microvilli by HNF4α. EBP50-deficient mice possess not only disorganized and shortened microvilli in the intestine but also concomitant reduction in phosphorylated ERM proteins at the apical membranes of polarized epithelia (Morales, et al., 2004), further supporting our conclusion.

Furthermore, we have shown that tRA induces the expression of ezrin but not radixin, moesin, or EBP50 in WT F9 cells. Up-regulation of ezrin by tRA in F9 cells has also been recently reported (Komiya et al., 2005). Nevertheless, tRA faintly caused the phosphorylation of ERM proteins and microvillus formation in WT F9 cells compared with those in Dox-treated F9 L32T2:HNF4α cells. It is also noteworthy that neither the induction of ezrin expression nor the weak biogenesis of microvilli was observed in the tRA-exposed RXRα$^{-/-}$/RARγ$^{-/-}$ cells, revealing that retinoid-induced events were definitely mediated by these retinoid receptors. Importantly, phosphorylation and apical enrichment of ERM proteins as well as microvillus formation were much more strikingly initiated when EBP50-overexpressed F9 cells were treated with tRA than those in the vehicle-treated transfectants and the tRA-exposed nontransfectants. Thus, in addition to EBP50 up-regulation, other molecules that are also induced by tRA are most likely necessary for the HNF4α-provoked activation of ERM proteins and microvillus biogenesis. It will be important in future studies to identify additional factors whose expression is induced by both HNF4α and retinoid receptors that trigger microvillus morphogenesis.

In summary, we have provided evidence showing that HNF4α functions as a robust morphogen to activate ERM proteins and provoke microvillus formation via the induction of EBP50 expression. The F9 L32T2:HNF4α cell line, like F9 L32T2, allows various experimental manipulations, such as tamoxifen-dependent Cre-mediated recombination, inducible gene expression (Chiba et al., 2000), and RNA interference (this study). In addition, it can be differentiated simply upon the addition of Dox from nonepithelial cells into polarized epithelial cells harboring prominent microvilli and mature junctional complexes (Chiba et al., 2003; Satohisa et al., 2005; and this study). Thus, the F9 L32T2:HNF4α cell line is definitely a powerful system that can be used to investigate molecular mechanisms underlying the process of epithelial polarization.

Materials and methods

Antibodies

Rat mAbs against ezrin, radixin, and moesin were purchased from Sanko Junyaku. Rabbit pAbs against EBP50, phospho–ezrin (Thr567)/radixin (Thr564)/moesin (Thr558), and actin were obtained from Affinity BioReagents, Inc., Cell Signaling Technology, and Sigma-Aldrich, respectively. A goat pAb against villin was purchased from Santa Cruz Biotechnology, Inc. The secondary antibodies used were as follows: HRP-conjugated anti–rat, anti–rabbit, or anti–goat IgG (DakoCytomation), AlexaFluor488 (green)-labeled anti–rabbit or anti–goat IgG (Invitrogen), AlexaFluor594 (red)-labeled anti–rabbit IgG (Invitrogen), and FITC-conjugated anti–rat IgG (DakoCytomation).

Cell lines and cell culture

The F9 mouse embryonal carcinoma cell line F9 L32T2, which exhibits both Dox-inducible gene expression (Tet-on; Gossen et al., 1995) and tamoxifen-dependent Cre-mediated recombination (Metzger and Chambon, 2001) systems, was generated as described previously (Chiba et al., 2000). To establish F9 cells expressing Dox-induced HNF4α (F9 L32T2:HNF4α), F9 L32T2 cells were electroporated with the expression vector pUHD10-3-rHNF4α, in which the expression of rHNF4α1 is under the control of the Tet operator along with the puromycin-resistant gene expression vector pHRLpuro1 (Chiba et al., 1997a) as described previously (Chiba et al., 2003, 2005). RXRα$^{-/-}$/RARγ$^{-/-}$ F9 cells were generated as reported previously (Chiba et al., 1997a).

A Tet-on system in RLE cells was established as for F9 cells (Chiba et al., 2000), and it was designated the RLE:rtTA L20 cell line as described previously (Fujibe et al., 2004). Cells showing the Dox-inducible expression of HNF4α were generated as described previously (Chiba et al., 2005).

Cells were plated in DME supplemented with 10% heat-inactivated FBS (Sanko Junyaku), 100 U/ml penicillin, and 100 μg/ml streptomycin and were treated with the vehicle, Dox, or retinoic acid 1 d after plating. The medium was changed every 2 d.

Electron microscopy

For scanning electron microscopy, cells grown on coverslips were fixed with 2.5% glutaraldehyde in PBS overnight at 4°C. After several rinses with PBS, they were postfixed in 1% OsO_4 at 4°C for 3 h and washed with distilled water followed by being dehydrated through a graded series of ethanol and freeze drying. Samples were subsequently coated with platinum and examined under a scanning electron microscope (S-4300; Hitachi).

For transmission electron microscopy, cells were fixed with 2.5% glutaraldehyde and 0.1 M cacodylate buffer, pH 7.3, overnight at 4°C. After washing with 0.1 M cacodylate buffer, pH 7.3, they were postfixed in 1% OsO_4 and 1.5% potassium ferrocyanide in 0.1 M cacodylate buffer for 2 h. Samples were subsequently stained with uranyl acetate for 2 h at room temperature, washed, and dehydrated followed by embedding in Epon 812. Ultrathin sections were cut with a diamond knife, stained with lead citrate, and examined with an electron microscope (1200Ex; JEOL) at an acceleration voltage of 100 kV.

RNA extraction and RT-PCR

For analysis of gene expression, total RNA was isolated from cells using TRIzol reagent (Invitrogen), and RT-PCR was performed as previously described (Chiba et al., 1997b, 2003; Satohisa et al., 2005). The PCR primers for mouse cDNAs were as follows: ezrin (GenBank/EMBL/DDBJ accession no. NM_009510), 5′-AGAGTACACGGCCAAGATC-3′ (nt 1,361–1,379) and 5′-TCTACATGGCCTCGAACTC-3′ (nt 1,839–1,857); radixin (GenBank/EMBL/DDBJ accession no. NM_009041), 5′-AAGCCAAGTCTGCAATCGC-3′ (nt 1,358–1,376) and 5′-TTGCCTTGTCGAATCTGCC-3′ (nt 1,862–1,880); moesin (GenBank/EMBL/DDBJ accession no. NM_0010833), 5′-GAACTTGAGCAGGAACGGA-3′ (nt 1,087–1,105) and 5′-CAGTCGCATGTTCTCAGCA-3′ (nt 1,602–1,620); and EBP50 (GenBank/EMBL/DDBJ accession no. NM_0012030), 5′-AGGTCAATGGTGTCTGCA-3′ (nt 724–741) and 5′-CTTTAGCCACAGCCAAGGA-3′ (nt 1,104–1,122). The primers for 36B4 were described previously (Kubota et al., 2001).

To confirm that amplifications were in the linear range, PCR was performed using three different numbers of cycles between 16 and 25, depending on the gene analyzed. Aliquots of PCR products were loaded onto 2% agarose gel and analyzed after staining with ethidium bromide.

Gel electrophoresis and immunoblotting

Cells were grown on 60-mm tissue culture plates, washed twice with ice-cold PBS, and scraped with 150 μl of ice-cold $NaHCO_3$ buffer (1 mM

$NaHCO_3$ and 1 mM PMSF, pH 7.5). They were subsequently collected into a microcentrifuge tube, sonicated for 10 s, and put on ice for 30 min. Total cell lysates were resolved by one-dimensional SDS-PAGE and electrophoretically transferred onto a polyvinylidene difluoride membrane (Immobilon; Millipore). The membrane was saturated with PBS containing 4% skim milk and incubated for 1 h at room temperature with primary antibodies in PBS. After rinsing in PBS containing 0.1% Tween 20, the membrane was incubated for 1 h at room temperature with HRP-conjugated anti–rat or anti–rabbit IgG (diluted 1:1,000) in PBS. For the detection of phospho-ERM proteins, TBS was used instead of PBS, and 5% BSA with 0.1% Tween 20 in TBS was used as a blocking buffer. It was then rinsed again and finally reacted using an ECL Western blotting detection system (GE Healthcare). The blots were stripped with Restore Western blot stripping buffer (Pierce Chemical Co.) according to the manufacturer's instructions and immunoprobed with an antiactin antibody. Signals in immunoblots were quantified using Image 1.62c software (Scion).

Immunohistochemistry

Cells grown on coverslips were fixed in 1% formaldehyde in PBS for 10 min. After being washed three times with PBS, they were treated with 0.2% Triton X-100 in PBS for 10 min, rinsed again with PBS, and preincubated in PBS containing 5% skim milk. They were subsequently incubated for 1 h at room temperature with primary antibodies and/or rhodamine phalloidin and rinsed again with PBS followed by a reaction for 1 h at room temperature with appropriate secondary antibodies. For immunohistochemistry of phospho-ERM proteins, TBS was used instead of PBS, and 5% BSA in TBS was used as a blocking solution. All samples were examined using a laser-scanning confocal microscope (MRC 1024; Bio-Rad Laboratories) and a planApo 60× NA 1.40 oil immersion objective (Nikon). Photographs were recorded with a computer (PowerEdge 2200; Dell) and OS/2 Warp software (IBM) and were processed with Photoshop 6.0 (Adobe). Observations were made at room temperature.

RNAi and transfection

Stealth siRNA duplex oligonucleotides against mouse EBP50 were synthesized by Invitrogen. The sequences were as follows: EBP50 RNAi #1, sense (5′-GGACCGAAUUGUGGAGGUCAAUGGU-3′) and antisense (5′-ACCAUUGACCUCCACAAUUCGGUCC-3′); EBP50 RNAi #2, sense (5′-CCAGCGAUACCAGUGAGGAGCUAAA-3′) and antisense (5′-UUUAGCUCCUCACUGGUAUCGCUGG-3′); and EBP50 RNAi #3, sense (5′-UACCAGUGAGGAGCUAAAUUCCCAA-3′) and antisense (5′-UUGGGAAUUUAGCUCCUCACUGGUA-3′). Cells were transfected with 100 pmol siRNAs or Stealth RNAi negative control by using LipofectAMINE 2000 reagent (Invitrogen) according to the manufacturer's protocols and were treated 6 h after transfection followed by exposure to Dox. For transient transfection of EBP50 cDNA, cells were transfected with the empty vector or pEGFP-EBP50 (provided by T. Shibata, National Cancer Research Institute, Tokyo, Japan; Shibata et al., 2003) by using LipofectAMINE 2000 reagent and were treated for 6 h after transfection followed by culture in the presence or absence of tRA.

Online supplemental material

Fig. S1 shows the effects of HNF4α and retinoic acid on villin expression in F9 monolayers. Fig. S2 shows the staining pattern of ERM protein, EBP50, and villin in RLE cells expressing Dox-induced HNF4α. Fig. S3 shows the staining pattern of ezrin and villin and scanning electron microscope images in EBP50-transformed F9 cells and nontransfectants that were treated with either the vehicle or tRA. Online supplemental material is available at http://www.jcb.org/cgi/content/full/jcb.200608012/DC1.

We are grateful to Dr. T. Shibata for providing the pEGFP-EBP50 expression vector; E. Suzuki, K. Takeda, and M. Nakazawa for their technical assistance; and K. Barrymore for help with the manuscript.

This work was supported by Grants-in-Aid from the Ministry of Education, Culture, Sports, Science and Technology of Japan.

Submitted: 2 August 2006
Accepted: 15 November 2006

References

Battle, M.A., G. Konopka, F. Parviz, A.L. Gaggl, C. Yang, F.M. Sladek, and S.A. Duncan. 2006. Hepatocyte nuclear factor 4α orchestrates expression of cell adhesion proteins during the epithelial transformation of the developing liver. *Proc. Natl. Acad. Sci. USA*. 103:8419–8424.

Bretscher, A. 1983. Purification of an 80,000-dalton protein that is a component of the isolated microvillus cytoskeleton, and its localization in nonmuscle cells. *J. Cell Biol.* 97:425–432.

Bretscher, A., K. Edwards, and R.G. Fehon. 2002. ERM proteins and merlin: integrators at the cell cortex. *Nat. Rev. Mol. Cell Biol.* 3:586–599.

Chiba, H., J. Clifford, D. Metzger, and P. Chambon. 1997a. Specific and redundant functions of retinoid X receptor/retinoic acid receptor heterodimers in differentiation, proliferation, and apoptosis of F9 embryonal carcinoma cells. *J. Cell Biol.* 139:735–747.

Chiba, H., J. Clifford, D. Metzger, and P. Chambon. 1997b. Distinct retinoid X receptor-retinoic acid receptor heterodimers are differentially involved in the control of expression of retinoid target genes in F9 embryonal carcinoma cells. *Mol. Cell. Biol.* 17:3013–3020.

Chiba, H., D. Metzger, and P. Chambon. 2000. F9 embryonal carcinoma cells engineered for tamoxifen-dependent Cre-mediated site-directed mutagenesis and doxycycline-inducible gene expression. *Exp. Cell Res.* 260:334–339.

Chiba, H., T. Gotoh, T. Kojima, S. Satohisa, K. Kikuchi, M. Osanai, and N. Sawada. 2003. Hepatocyte nuclear factor (HNF)-4α triggers formation of functional tight junctions and establishment of polarized epithelial morphology in F9 embryonal carcinoma cells. *Exp. Cell Res.* 286:288–297.

Chiba, H., T. Itoh, S. Satohisa, N. Sakai, H. Noguchi, M. Osanai, T. Kojima, and N. Sawada. 2005. Activation of $p21^{CIP1/WAF1}$ gene expression and inhibition of cell proliferation by overexpression of hepatocyte nuclear factor-4α. *Exp. Cell Res.* 302:11–21.

D'Alterio, C., D.D.D. Tran, M.W.Y. Au Yeung, M.S.H. Hwang, M.A. Li, C.J. Arana, V.K. Mulligan, M. Kubesh, P. Sharma, M. Chase, et al. 2005. *Drosophila melanogaster* Cad99C, the orthologue of human Usher cadherin PCDH15, regulates the length of microvilli. *J. Cell Biol.* 171:549–558.

DeRosier, D.J., and L.G. Tilney. 2000. F-actin bundles are derivatives of microvilli: what does this tell us about how bundles might form? *J. Cell Biol.* 148:1–6.

Doi, Y., M. Itoh, S. Yonemura, H. Ishihara, T. Takano, T. Noda, and S. Tsukita. 1999. Normal development of mice and unimpaired cell adhesion/cell motility/actin-based cytoskeleton without compensatory up-regulation of ezrin or radixin in moesin gene knockout. *J. Biol. Chem.* 274:2315–2321.

Donowitz, M., B. Cha, C. Zachos, C.L. Brett, A. Sharma, M. Tse, and X. Li. 2005. HHERF family and NHE3 regulation. *J. Physiol.* 567:3–11.

Duncan, S.A., K. Manova, W.S. Chen, P. Hoodless, D.C. Weinstein, R.F. Bachvarova, and J.E. Darnell Jr. 1994. Expression of transcription factor HNF-4 in the extraembryonic endoderm, gut, and nephrogenic tissue of the developing mouse embryo: HNF-4 is a marker for primary endoderm in the implanting blastocyst. *Proc. Natl. Acad. Sci. USA*. 91:7598–7602.

Ferrary, E., M. Cohen-Tannoudji, G. Pehau-Arnaudet, A. Lapillonne, R. Athman, T. Ruiz, L. Boulouha, F. El Marjou, A. Doye, J.-J. Fontaine, et al. 1999. In vivo, villin is required for Ca^{2+}-dependent F-actin disruption in intestinal brush borders. *J. Cell Biol.* 146:819–829.

Finnerty, C.M., D. Chambers, J. Ingraffea, H.R. Faber, P.A. Karplus, and A. Bretscher. 2004. The EBP50-moesin interaction involves a binding site regulated by direct masking on the FERM domain. *J. Cell Sci.* 117:1547–1552.

Frolenkov, G.I., I.A. Belyantseva, T.B. Friedman, and A.J. Griffith. 2004. Genetic insight into the morphogenesis of inner ear hair cells. *Nat. Rev. Genet.* 5:489–498.

Fujibe, M., H. Chiba, T. Kojima, T. Soma, T. Wada, T. Yamashita, and N. Sawada. 2004. Thr203 of claudin-1, a putative phosphorylation site for MAP kinase, is required to promote the barrier function of tight junctions. *Exp. Cell Res.* 295:36–47.

Gary, R., and A. Bretscher. 1995. Ezrin self-association involves binding of an N-terminal domain to a normally masked C-terminal domain that includes the F-actin binding sites. *Mol. Biol. Cell*. 6:1061–1075.

Gossen, M., S. Freundlieb, G. Bender, G. Müller, W. Hllen, and H. Bujard. 1995. Transcriptional activation by tetracyclines in mammalian cells. *Science*. 268:1766–1769.

Hayhurst, G.P., Y.H. Lee, G. Lambert, J.M. Ward, and F.J. Gonzalez. 2001. Hepatocyte nuclear factor 4α (nuclear receptor 2A1) is essential for maintenance of hepatic gene expression and lipid homeostasis. *Mol. Cell. Biol.* 21:1393–1403.

Hogan, B.L., A. Taylor, and E. Adamson. 1981. Cell interactions modulate embryonal carcinoma cell differentiation into parietal or visceral endoderm. *Nature*. 291:235–237.

Kikuchi, S., M. Hata, K. Fukumoto, Y. Yamane, T. Matsui, A. Tamura, S. Yonemura, H. Yamagishi, D. Keppler, Sh. Tsukita, and Sa. Tsukita. 2002. Radixin deficiency causes conjugated hyperbilirubinemia with loss of Mrp2 from bile canalicular membranes. *Nat. Genet.* 31: 320–325.

Komiya, S., M. Shimizu, J. Ikenouchi, S. Yonemura, T. Matsui, Y. Fukunaga, H. Liu, S. Tsukita, and A. Nagafuchi. 2005. Apical membrane and junctional complex formation during simple epithelial cell differentiation. *Genes Cells*. 10:1065–1080.

Kubota, H., H. Chiba, Y. Takakuwa, M. Osanai, H. Tobioka, G. Kohama, M. Mori, and N. Sawada. 2001. Retinoid X receptor α and retinoic acid receptor γ mediate expression of genes encoding tight junction proteins and barrier function in F9 cells during visceral endodermal differentiation. *Exp. Cell Res.* 263:163–172.

Lankes, W., A. Griesmacher, J. Grunwald, R. Schwartz-Albiez, and R. Keller. 1988. A heparin-binding protein involved in inhibition of smooth-muscle cell proliferation. *Biochem. J.* 251:831–842.

Lazarevich, N.L., O.A. Cheremnova, E.V. Varga, D.A. Ovchinnikov, E.I. Kudrjavtseva, O.V. Morozova, D.I. Fleishman, N.V. Engelhardt, and S.A. Duncan. 2004. Progression of HCC in mice is associated with a down-regulation in the expression of hepatocyte nuclear factors. *Hepatology*. 39:1038–1047.

Li, J., G. Ning, and S.A. Duncan. 2000. Mammalian hepatocyte differentiation requires the transcription factor HNF-4α. *Genes Dev.* 14:464–474.

Lucas, B., K. Grigo, S. Erdmann, J. Lausen, L. Klein-Hitpass, and G.U. Ryffel. 2005. HNF4α reduces proliferation of kidney cells and affects genes deregulated in renal cell carcinoma. *Oncogene*. 24:6418–6431.

Mangeat, P., C. Roy, and M. Martin. 1999. ERM proteins in cell adhesion and membrane dynamics. *Trends Cell Biol.* 9:187–192.

Matsui, T., M. Maeda, Y. Doi, S. Yonemura, M. Amano, K. Kaibuchi, and S. Tsukita. 1998. Rho-kinase phosphorylates COOH-terminal threonines of ezrin/radixin/moesin (ERM) proteins and regulates their head-to-tail association. *J. Cell Biol.* 140:647–657.

Metzger, D., and P. Chambon. 2001. Site- and time-specific gene targeting in the mouse. *Methods*. 24:71–80.

Morales, F.C., Y. Takahashi, E.L. Kreimann, and M.-M. Georgescu. 2004. Ezrin-radixin-moesin (ERM)-binding phosphoprotein 50 organizes ERM proteins at the apical membrane of polarized epithelia. *Proc. Natl. Acad. Sci. USA*. 101:17705–17710.

Parviz, F., C. Matullo, W.D. Garrison, L. Savatski, J.W. Adamson, G. Ning, K.H. Kaestner, J.M. Rossi, K.S. Zaret, and S.A. Duncan. 2003. Hepatocyte nuclear factor 4α controls the development of a hepatic epithelium and liver morphogenesis. *Nat. Genet.* 34:292–296.

Pearson, M.A., D. Reczek, A. Bretscher, and P.A. Karplus. 2000. Structure of ERM protein moesin reveals the FERM domain fold masked by an extended actin binding tail domain. *Cell*. 101:259–270.

Pinson, K.I., L. Dunbar, L. Samuelson, and D.L. Gumucio. 1998. Targeted disruption of the mouse villin gene does not impair the morphogenesis of microvilli. *Dev. Dyn.* 211:109–121.

Reczek, D., and A. Bretscher. 1998. The carboxyl-terminal region of EBP50 binds to a site in the amino-terminal domain of ezrin that is masked in the dormant molecule. *J. Biol. Chem.* 273:18452–18458.

Reczek, D., M. Berryman, and A. Bretscher. 1997. Identification of EBP50: a PDZ- containing phosphoprotein that associates with members of the ezrin-radixin-moesin family. *J. Cell Biol.* 139:169–179.

Saotome, I., M. Curto, and A.I. McClatchey. 2004. Ezrin is essential for epithelial organization and villus morphogenesis in the developing intestine. *Dev. Cell*. 6:855–864.

Satohisa, S., H. Chiba, M. Osanai, S. Ohno, T. Kojima, T. Saito, and N. Sawada. 2005. Behavior of tight-junction, adherens-junction and cell polarity proteins during HNF-4α-induced epithelial polarization. *Exp. Cell Res.* 310:66–78.

Schlichting, K., M. Wilsch-Brauninger, F. Demontis, and C. Dahmann. 2006. Cadherin Cad99C is required for normal microvilli morphology in *Drosophila* follicle cells. *J. Cell Sci.* 119:1184–1195.

Shibata, T., M. Chuma, A. Kokubu, M. Sakamoto, and S. Hirohashi. 2003. EBP50, a β-catenin-associating protein, enhances Wnt signaling and is over-expressed in hepatocellular carcinoma. *Hepatology*. 38:178–186.

Sladek, F.M., and S.D. Seidel. 2001. Hepatocyte nuclear factor 4α. *In* Nuclear Receptors and Genetic Disease. T.P. Burris and E.R.B. McCabe, editors. Academic Press, San Diego, CA. 309–361.

Sladek, F.M., W. Zhong, E. Lai, and I.E. Darnel. 1990. Liver-enriched transcription factor HNF-4 is a novel member of the steroid hormone receptor superfamily. *Genes Dev.* 4:2353–2365.

Späth, G.F., and M.C. Weiss. 1998. Hepatocyte nuclear factor 4 provokes expression of epithelial marker genes, acting as a morphogen in dedifferentiated hepatoma cells. *J. Cell Biol.* 140:935–946.

Strickland, S. 1981. Mouse teratocarcinoma cells: prospects for the study of embryogenesis and neoplasia. *Cell*. 24:277–278.

Takeuchi, K., N. Sato, H. Kasahara, N. Funayama, A. Nagafuchi, S. Yonemura, Sa. Tsukita, and Sh. Tsukita. 1994. Perturbation of cell adhesion and microvilli formation by antisense oligonucleotides to ERM family members. *J. Cell Biol.* 125:1371–1384.

Tamura, A., S. Kikuchi, M. Hata, T. Katsuno, T. Matsui, H. Hayashi, Y. Suzuki, T. Noda, Sh. Tsukita, and Sa. Tsukita. 2005. Achlorhydria by ezrin knockdown: defects in the formation/expansion of apical canaliculi in gastric parietal cells. *J. Cell Biol.* 169:21–28.

Tirona, R.G., W. Lee, B.F. Leake, L.B. Lan, C.B. Cline, V. Lamda, F. Parviz, S.A. Duncan, Y. Inoue, F.J. Gonzalez, et al. 2003. The orphan nuclear receptor HNF4α determines PXR- and CAR-mediated xenobiotic induction of CYP3A4. *Nat. Med.* 9:220–224.

Tsukita, S., and S. Yonemura. 1999. Cortical actin organization: lessons from ERM (ezrin/radixin/moesin) proteins. *J. Biol. Chem.* 274:34507–34510.

Tsukita, Sa., Y. Hieda, and Sh. Tsukita. 1989. A new 82-kD barbed end-capping protein (radixin) localized in the cell-to-cell adherens junction: purification and characterization. *J. Cell Biol.* 108:2369–2382.

Watt, A.J., W.D. Garrison, and S.A. Duncan. 2003. HNF4: a central regulator of hepatocyte differentiation and function. *Hepatology*. 37:1249–1253.

Weinman, E.J., D. Steplock, Y. Wang, and S. Shenolikar. 1995. Characterization of a protein co-factor that mediates protein kinase A regulation of the renal brush border membrane Na^+/H^+ exchange. *J. Clin. Invest.* 95:2143–2149.